

Atomic collisions with relativistic heavy ions. VII. *L*- and *M*-shell electron stripping of ions in light targets

W. E. Meyerhof, R. Anholt, and Xiang-Yuan Xu*

Department of Physics, Stanford University, Stanford, California 94305

(Received 28 August 1986)

The charge distribution of many-electron ions (Xe,U) moving with relativistic velocities through light target foils is examined. In these targets, electron capture into the *L* and *M* shells of the ion and multiple ionization are negligible compared to one-electron stripping. Using a simple model for the stripping cross section, we show that a universal analytical expression can then be obtained for the target-thickness dependence of each charge fraction of the ion. This expression gives insight into the statistical nature of the stripping process and allows the extraction of one-electron ionization cross sections.

I. INTRODUCTION

Other papers in this series considered ionization and capture processes in relativistic heavy ions (II–V, VIII) (Refs. 1–5) with the ultimate aim of being able to predict *ab initio* the charge states of relativistic ions in matter. Unlike low-velocity, many-electron ions in matter,⁶ relativistic heavy ions have high velocities relative to the Bohr velocities of ionized electrons, allowing one to apply high-velocity theories like the plane-wave Born approximation (PWBA) (Ref. 7) to ionization and the eikonal approximation⁸ to capture. We have concentrated on high-*Z*, few-electron ions where many-electron wave functions need not be used, although Dirac (hydrogenic) wave functions are usually required for the inner-shell electrons.

One of the major obstacles to developing a complete theory of ions in matter is to delineate the role of excited states in determining the overall charge states of ions in matter. Bohr and Linhard⁹ pointed out that due to the more rapid rate of excitation of ions in matter compared to their decay, electrons spend a high fraction of time in excited states where they are more easily excited, leading to larger effective ionization cross sections. With zero-, one-, and two-electron relativistic heavy ions, we were able to develop the first *ab initio* model of the states of ions in matter incorporating these excited-state effects.^{1,4}

Despite the significant simplifications proffered by studying relativistic heavy ions, when one turns attention to ions with more electrons than two, the level of complication grows so steeply that further progress requires the abandonment of many-state models in favor of simplified ones. With the eleven-state model described in V, dozens of cross sections were needed to explain the states of just two-electron ions in matter.⁴ In many-electron systems, the fundamental cross sections are more difficult to calculate, since they require many-electron wave functions, and many more are needed. In addition, we have recently identified important multiple-electron ionization and capture processes, making the required number of cross sections even larger.^{5,10}

Nevertheless, we have discovered that for certain collision systems, one can still develop simple and indeed analytical models of the states of as many as 24-electron ions in matter. One has to restrict consideration to collisions of relativistic many-electron ions in low-*Z* targets. In these collisions, capture processes are unimportant compared to ionization ones, except possibly for the *K* shell. Also, since the cross sections for the simultaneous loss of *m* projectile electrons relative to the single-electron loss (*m*=1) varies as $(Z_t/Z_p)^{2m}$, where Z_t and Z_p ($\gg Z_t$) are the target and projectile atomic numbers, respectively, we can neglect them.¹⁰ Denoting the cross section for changing the number of electrons on the projectile from n_i to $n_f = n_i - 1$ by $\sigma(n_i, n_f)$, the rate equations for the charge-state fractions $Y_n(T)$ at a thickness T (in atoms/cm²) are^{6,11}

$$dY_n/dT = \sum_{\substack{n' \\ (n' \neq n)}} [\sigma(n', n)Y_{n'} - \sigma(n, n')Y_n] \quad (1a)$$

$$= \sigma(n+1, n)Y_{n+1} - \sigma(n, n-1)Y_n, \quad (1b)$$

where $\sum_n Y_n = 1$. In Eq. (1a), cross sections per atom for $n' < n$ are called loss cross sections and for $n' > n$ attachment cross sections which along with multiple-ionization ones, are neglected in Eq. (1b). The essential approximation made here is that excited-state effects are relatively small, so that the loss cross sections can be interpreted in terms of fundamental ionization cross sections or at least in terms of "effective cross sections."⁴

Section II of this paper discusses the cross sections needed in Eq. (1b), and Sec. III discusses an analytical solution to Eq. (1b) that can be compared with experiment and, furthermore, can be used in fitting procedures to extract cross sections from data. The model is compared with measurements of charge states of incident 82- to 300-MeV/amu Xe⁴⁵⁺ and 100- to 962-MeV/amu U⁶⁸⁺ and U⁸³⁺ ions traversing Be, C, Mylar, and Al foils.^{3,5,12} Section V contains the conclusions, and Appendix A de-

scribes how the PWBA was applied to calculate the fundamental ionization cross sections compared with experiment in Sec. IV.

II. ELECTRON-LOSS CROSS SECTION

We denote the single-electron loss or stripping cross section for an n -electron ion by s_n ; it is related to the single-electron ionization cross section in shell k , called σ_i^k , as shown below. In terms of the cross section used in Eq. (1), s_n is given by

$$s_n = \sigma(n, n-1). \quad (2)$$

Gould has extracted single-electron-loss cross sections from charge distributions of 962-MeV/amu Fe¹⁶⁺ and U⁶⁸⁺ projectiles traversing various thicknesses of Mylar and C foils, henceforth abbreviated by C(My).¹² He used a least-squares-fitting program for Eq. (1), originally developed by Betz, and described in Refs. 6 and 13. Figures 1(a)–1(c) show the cross sections s_n plotted as a function of the number of electrons in the K and L shells of Fe and the M shell of U, respectively. One sees an approximately linear dependence on n as each major shell k ($k=K, L, M$) is stripped of electrons. Hence, we assume that within each major shell the contribution to the one-electron-loss cross section is proportional to the number of electrons n_k in the shell. This results in expressions for M -shell stripping,

$$s_n = n_M \sigma_i^M + 8\sigma_i^L + 2\sigma_i^K, \quad n = n_M + 10 \quad (3a)$$

for L -shell stripping,

$$s_n = n_L \sigma_i^L + 2\sigma_i^K, \quad n = n_L + 2 \quad (3b)$$

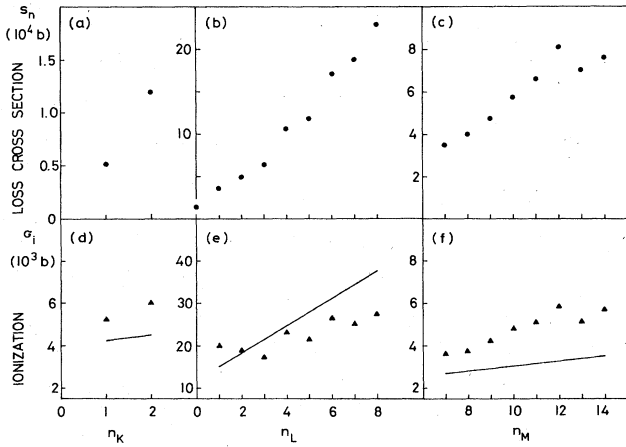


FIG. 1. K -, and L -, and M -shell loss [(a)–(c)] and ionization [(d)–(f)] cross sections for 962-MeV/amu Fe [(a), (b), (d), and (e)] and U [(c) and (f)] traversing C(My) foils. The loss cross sections were obtained by Gould (Ref. 12) with an estimated error of a factor of 2. The ionization cross sections were obtained from expressions (7a) to (7c) for the M shell of U and the L and K shells of Fe, respectively. The number of electrons in these shells are denoted by n_M , n_L , and n_K , respectively. The curves in (d)–(f) are PWBA predictions (see the Appendix).

and for K -shell stripping,

$$s_n = n_K \sigma_i^K, \quad n = n_K. \quad (3c)$$

Below, we discuss the influence of changing screening as each shell is stripped.

The basic assumption, that within each major shell the contribution to the loss cross section is proportional to the number of electrons left in the shell, can be understood theoretically in the following way (see Sec. 3.2 of Ref. 11). If $P_{ik}(b)$ is the average ionization probability per electron in the shell k at an impact parameter b ,

$$P_{ik}(1 - P_{ik})^{n_k - 1}, \quad (4)$$

is the probability that only one given electron is ionized among the n_k electrons. Hence, the contribution to the single-electron-loss cross section from the shell k is

$$n_k \int_0^\infty db 2\pi b P_{ik}(1 - P_{ik})^{n_k - 1}. \quad (5)$$

If, in the important range of impact parameters, $P_{ik} \ll 1$, one can approximate expression (5) by

$$n_k \int db 2\pi b P_{ik} = n_k \sigma_i^k, \quad (6)$$

which is the expression used in Eqs. (3). In another publication, we discuss examples where P_{ik} is not negligibly small compared to unity.¹⁰

To check experimentally whether σ_i^k varies with n_k , i.e., with varying screening, one can proceed as follows. Using the cross sections s_n shown in Figs. 1(a)–1(c) and estimating σ_i^K and σ_i^L from a relativistic ionization calculation (see the Appendix),^{7,14} one can derive average one-electron ionization cross sections from Eqs. (3a)–(3c) as follows:

$$\langle \sigma_i^M \rangle = (s_n - 8\sigma_i^L - 2\sigma_i^K) / n_M \quad \text{for } n > 10, \quad (7a)$$

$$\langle \sigma_i^L \rangle = (s_n - 2\sigma_i^K) / n_L \quad \text{for } 2 < n \leq 10, \quad (7b)$$

$$\langle \sigma_i^K \rangle = s_n / n_K \quad \text{for } n \leq 2. \quad (7c)$$

Figures 1(d)–1(f) give the results for expressions (7) as a function of N_K , N_L , and n_M , respectively. For each shell, one can see an increase of σ_i^k with increasing n_k . This is expected theoretically, since increased screening gives smaller electron binding energies, and, hence, should increase the ionization cross section. To check this, one can equate, for each shell, the electron binding energies to the relevant ionization potentials for stripped ions computed by Carlson *et al.*¹⁵ Then, using the relativistic ionization theory (see the Appendix),^{7,14} one obtains the lines shown in Figs. 1(d)–1(f). These calculated cross sections have the same trends as the semiempirical expressions (7a)–(7c), although not exactly the same magnitudes, presumably due to excited-state effects.⁴ Hence, within each shell, we assume a linear variation of σ_i^k with n_k :

$$\sigma_i^k(n_k) = \sigma_i^k(1) + (n_k - 1)\Delta\sigma_i^k, \quad (8)$$

where

$$\Delta\sigma_i^k = \{\sigma_i^k[n_k(\text{max})] - \sigma_i^k(1)\} / [n_k(\text{max}) - 1]. \quad (9)$$

In Eq. (9), $n_k(\text{max})$ is the maximum number of electrons which can occupy shell k .

III. UNIVERSAL STRIPPING MODEL

A. Ion with a single shell

We start by presenting a schematic model which shows very clearly that charge distributions are determined essentially by statistical processes. Following Eq. (6), let us make the oversimplified assumption that on the average the one-electron loss cross section for an n -electron ion is proportional to n :

$$s_n = n\sigma_i, \quad (10)$$

where σ_i is a mean one-electron ionization cross section. Then, in traversing a target of thickness T , each electron has the same probability

$$\tau = \exp(-\sigma_i T) \quad (11)$$

of surviving on the ion, and the probability $(1-\tau)$ to be stripped. If the ion enters with N electrons into the target, the probability that n electrons survive after traversal of the target is just the binomial expression

$$Y_n = \left[\frac{N!}{n!(N-n)!} \right] \tau^n (1-\tau)^{N-n}. \quad (12)$$

This probability is the yield of the charge state with n electrons if the total yield is normalized to unity.

From Eq. (12), one can conclude that the mean charge of a projectile of atomic number Z_p at a given target thickness T is given by

$$Z_{\text{eff}} = Z_p - N\tau, \quad (13)$$

a quantity of interest in energy-loss considerations. Also one can easily show that each Y_n , except for $n=0$ and $n=N$, passes through a maximum at the target thickness T_m where

$$\tau_m = n/N \text{ or } T_m = [\ln(N/n)]/\sigma_i. \quad (14)$$

The peak value of Y_n is given by

$$Y_n(T_m) = \left[\frac{N!}{n!(N-n)!} \right] n^n (N-n)^{N-n} / N^N \quad (15)$$

$$\approx \left[\frac{N}{2\pi n(N-n)} \right]^{1/2}. \quad (16)$$

In Eq. (16), Stirling's approximation has been used for each factorial. One sees that, under the assumptions made, the maximum yield of a given charge fraction Y_n depends only on n and the initial number N of electrons, and is independent of the projectile energy, Z_p or Z_t . This is a useful fact to note, if one wishes to obtain maximum yield of a certain ionic species.

B. Analytical solution of the rate equations

To treat the more realistic case of stripping of an ion with different shells and different cross sections [Eq. (3)], one has to solve the rate equations (1) for the charge fractions. Neglecting attachment and multiple-electron loss, as in Eq. (1b), the rate equations are identical to those

which apply in the interior of an electron-beam ion source in which electron-ion recombination and ion losses are negligibly small. The solution for those rate equations has been given by Kostroun.¹⁶ Mathematically, the equations are the same as those for radioactive series decay, first solved by Bateman by the Laplace transform method.¹⁷ If a single charge fraction $Y_N(0)=1$ enters the target, the solutions of Eq. (1b) are

$$Y_n(T) = Y_N(0) \left[\prod_{j=n+1}^N s_j \right] \sum_{j=n}^N \left[\frac{e^{-s_j T}}{\prod_{\substack{i=n \\ (i \neq j)}}^N (s_i - s_j)} \right]. \quad (17)$$

Here, all cross sections s_j are single-electron-loss cross sections. The equilibrium fractions $F_n = Y_n(\infty)$ corresponding to the assumption of pure loss are, of course, $F_0=1$ and $F_{n \neq 0}=0$.

It is helpful to write Eq. (3) in a form similar to Eq. (10). For an atom with m electrons in a given shell, we write Eqs. (3) as follows:

$$s_m = (m+g)\sigma_i. \quad (18)$$

Essentially, the quantity of g corrects the stripping cross section for the presence of inner shells. By comparison with Eq. (3) one finds for the M shell, $\sigma_i = \sigma_i^M$ and

$$g = (8\sigma_i^L + 2\sigma_i^K) / \sigma_i^M; \quad (19)$$

for the L shell, $\sigma_i = \sigma_i^L$ and

$$g = 2\sigma_i^K / \sigma_i^L; \quad (20)$$

and for the K shell, $\sigma_i = \sigma_i^K$ and $g=0$. By substituting Eq. (18) into Eq. (17), one can show that within a given shell, the solutions to the rate equations still have the form of Eq. (12), but with the replacements on the right-hand side,

$$N \rightarrow M+g, \quad n \rightarrow m+g, \quad (21)$$

where M is the initial number and m is the emerging number of electrons in the shell. The initial condition $Y_M(0)=1$ still applies; otherwise, the solutions become considerably more complex.¹⁷ For electron stripping across several shells, one must use Eq. (17) directly. The final expression for the target-thickness dependence of the charge fraction in a given shell is, therefore,

$$Y_m = \left[\frac{(M+g)!}{[(m+g)!(M-m)!]} \right] \tau^{m+g} (1-\tau)^{M-m}, \quad (22)$$

where τ is given by Eq. (11).

C. Linearization of the charge fraction expression

If one tries to compare all the measured charge fractions as a function of target thickness with Eq. (22), one obtains a very busy or complicated figure, because the curves and the data for different values of m overlap. Hence, we searched for ways to "linearize" Eq. (22) and have found a simple way to do this. If one forms the ratio Y_m/Y_{m+1} at the same value T , one obtains from Eq. (22) with a little algebra the expression

$$\sigma_i = (1/T) \ln \left[\left(1 + \frac{M-m}{m+1+g} \right) \frac{Y_m}{Y_{m+1}} \right]. \quad (23)$$

Here σ_i is the ionization probability per electron in a given shell, as defined in Eq. (18).

By plotting σ_i against m for a given value of T (or against T , for a given value of m), one should, in principle, obtain the same constant value for σ_i . In practice, we expect an increase of σ_i with m due to screening effect [Figs. 1(e) and 1(f) and Eq. (8)], even though screening effects are not built into our model [see Eq. (18)].

IV. COMPARISON WITH EXPERIMENT

In order to compare Eqs. (22) or (23) with experiment, one must compute the inner-shell correction constants g defined in Eqs. (19) and (20). This can be done by using the relativistic PWBA described in the Appendix. One then finds for the collision systems of interest here typical values of $g \approx 2-3$ for the M shell and $g \approx 0.2-0.3$ for the L shell. [The larger value of g for the M shell is mainly due to the factor 8 in Eq. (19).] Except near the ends of a shell ($m \lesssim 2$), the computed values of Y_m (or of σ_i) are not very sensitive to the exact value of g . This is illustrated in Fig. 2, where curves for Y_m values τ are shown for $m = n_L = 0, 1, \text{ and } 2$, assuming $g = 0.2, 0.3, \text{ and } 0.4$. Experimental data for 82-, 140-, 200-, 300-MeV/amu Xe^{45+}

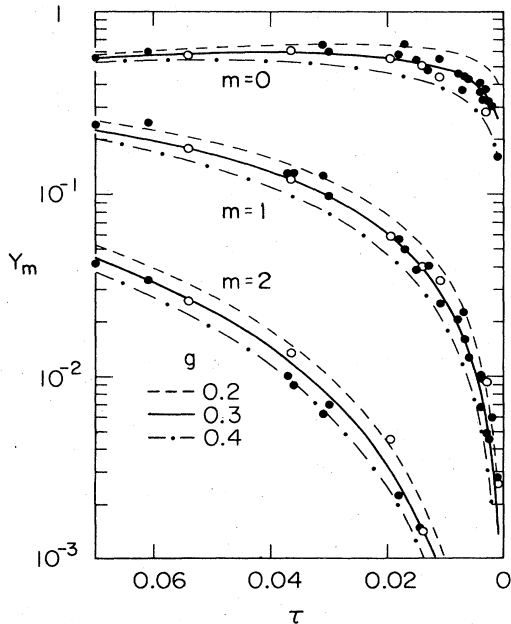


FIG. 2. Charge-state yields Y_m as a function of target-thickness parameter τ for large target thicknesses. The parameter τ is defined in Eq. (11). Target thicknesses increase to the right. Curves are shown for ($m=$)0-, 1-, and 2-electron ions, using $M=7$ and $g=0.2, 0.3, \text{ and } 0.4$ in Eq. (22). The data are for 82-, 140-, 200-, and 300-MeV/amu Xe^{45+} (closed symbols) and 105-, 430-, and 962-MeV/amu U^{83+} (open symbols) passing through C, Mylar, and Al targets.

stripped by Be, Mylar, and Al targets are given for comparison (the fitting procedure is discussed below).

A. Charge fractions

To give an indication of the universality of Eq. (22), we make a direct comparison with it for a few values of M and m , but the bulk of the available data are compared with Eq. (23). In the comparison with Eq. (22), the first step is to search for the optimum value of τ , which, at a given value of T , fits a plot of Y_m versus m . Figures 3 and 4 show such plots, one for L -shell stripping with $M=N_L=7$ and one for M -shell stripping with $M=N_M=14$. In principle, one could make least-squares searches for the best values of τ , but we chose to make a fit by eye, in order to take into account possible systematic errors in Y_m (e.g., incorrect background subtraction under experimental charge-state peaks).

Once the best value of τ has been found, first, one can extract σ_i by means of Eq. (11); second, one can put a data point on a plot of Y_m versus τ , such as that shown in Fig. 5. If Eq. (22) is indeed universal, the extracted values of σ_i for a given collisions system should be independent of T and all the Y_m data for a given set M, m should fall on universal curves of Y_m versus τ . Figure 5 gives sample plots for $M=N_L=7$ and $m=n_L=7, 5, \text{ and } 0$, using data from 82-, 220-, 430-, and 960-MeV/amu U^{83+} passing through targets of Be, C(My), and Al foils. The curves shown assume $g=0.3$. As noted previously, for $n_L=0$, the fit depends sensitively on the value of g chosen.

Figure 6 gives values of σ_i extracted via Eq. (11) from the best-fit values of τ at each target thickness (see sample plots in Figs. 3 and 4). Data were used from measurements with 962-MeV/amu $\text{U}^{68+} + \text{C(My)}$, Al, and 962-

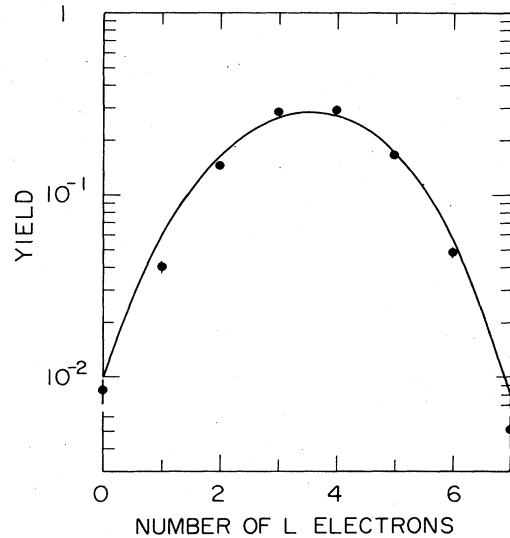


FIG. 3. Charge-state yields for 300-MeV/amu Xe^{45+} passing through a 2.52-mg/cm² Be target as a function of the resulting L -electron number on the ion. (The incident number of L electrons is $N_L=7$.) An optimum value of τ was chosen to produce the fit, assuming $g=0.3$ in Eq. (22).

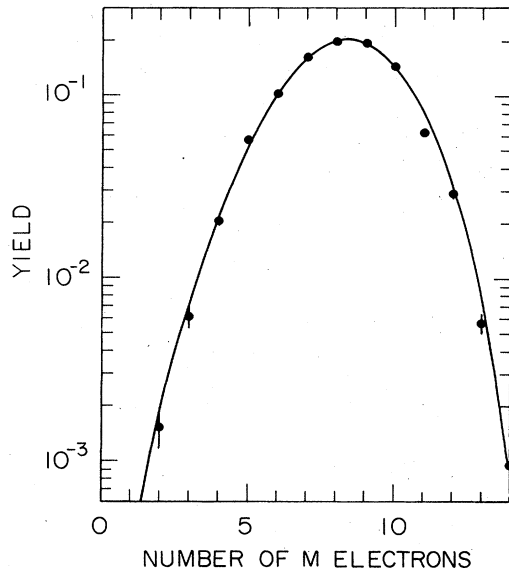


FIG. 4. Charge-state yields for 962-MeV/amu U^{68+} passing through a 1.77-mg/cm² Mylar foil as a function of the resulting number of M electrons on the ion. (The incident number of M electrons is $N_M=14$.) An optimum value of τ was chosen to produce the fit, assuming $g=3$ in Eq. (22).

MeV/amu $U^{83+} + \text{Be}$, C(My), Al collisions. From the U^{68+} data, a mean M -shell ionization cross section σ_i^M was obtained, and from the U^{83+} data, a mean L -shell cross section σ_i^L . To place the data on a common plot, the reduced cross sections $\sigma_i/(Z_i^2+Z_t)$ are given, where Z_t is the atomic number of the target [$Z_t(\text{My})=6.63$]. The

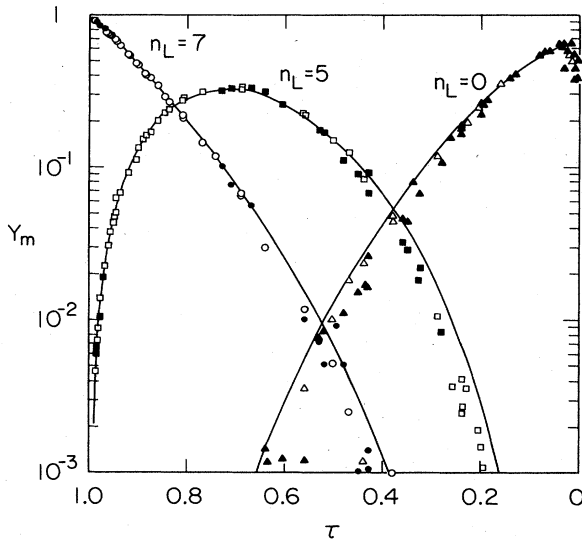


FIG. 5. Sample charge-state yields as a function of the target-thickness parameter τ , for 82-, 100-, 200-, and 300-MeV/amu Xe^{45+} (closed symbols) and 105-, 430-, and 960-MeV/amu U^{83+} (open symbols) passing through Be, C, Mylar, and Al targets. The curves are for an incident number of L electrons $N_L=7$, and are given for L -electron numbers $n_L=7$, 5, and 0, assuming $g=0.3$ in Eq. (22).

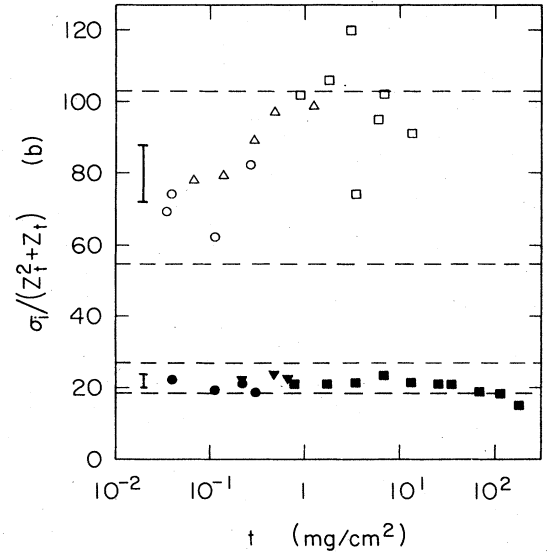


FIG. 6. Reduced one-electron ionization cross sections extracted from fits of measured charge-state fractions to the universal formula Eq. (22), as a function of target thickness. L -shell data from 962-MeV/amu $U^{83+} + \text{Be}$ (Δ), O (\bullet), and Mylar (\blacksquare). M -shell data from 962-MeV/amu $U^{68+} + \text{C}$ (\circ), Mylar (\square), and Al (\triangle). The dashed horizontal lines are PWBA predictions, assuming either one or the maximum number of electrons in each shell. Typical error bars are shown on the left-hand side of the figure.

fluctuations in the cross sections are probably due to uncertainties in the target thicknesses (typically, $\pm 10\%$) which enter into the computation of σ_i . One sees that the reduced L -shell cross section is nearly constant over a span of target thicknesses of 4 orders of magnitude, supporting the validity of Eq. (22). For the M shell, there appears to be an increase of the reduced cross section with target thickness, which may reflect the influence of screening or excited-state effects. Extreme screening variations across the L and M shells expected from the PWBA are indicated by the dotted horizontal lines in Figs. 6.

There is one slight inconsistency in our analysis, because, on the one hand, we compute g assuming that the cross sections σ_i for all the shells are known [Eqs. (19) and (20)], on the other hand, we extract σ_i from the fits like those of Figs. 3 and 4. In principle, one could make a self-consistent analysis by leaving not only τ , but also g , as free parameters in a global least-squares fit to all the data for a given shell. This effort did not seem worthwhile to us, because of the relative insensitivity of Y_m to g and the insufficient precision of the data, as well as of the target thickness.

B. Cross sections

Figures 3–6 indicate that to within a satisfactory accuracy Eq. (22) provides a universal description of the target-thickness dependence of charge fractions in collisions in which capture and multiple stripping are negligible. We can illustrate this point in a different way by

using Eq. (23) to extract σ_i directly from ratios of measured charge fractions. Here, the analysis is very simple. Once g has been computed for the collisions system and electron shell under consideration, Eq. (23) can be used directly. In Fig. 7, we give sample results for 962-MeV/amu $U^{68+} + My$ and $U^{83+} + My$ as a function of the number of electrons in the M and L shells, for various target thicknesses. On the whole, a satisfactory consistency in σ_i for each case is obtained. There is a slightly increasing trend of σ_i with the number of electrons in the shell, which probably reflects screening effects [Eq. (8)]. For comparison, we show the PWBA estimates for $\sigma_i(m)$.

V. CONCLUSIONS

We have shown that under certain conditions, a very simple description of the projectile charge fraction dependence on target thickness is possible. A universal expression can be derived essentially from statistical considerations. Our effort is complementary to that of Åberg and co-workers, who have derived a stochastic theory of *equilibrium* charge-state distributions.^{18–20} Their theory contains an arbitrary parameter (called α in Refs. 19 and 20) whose values, in our opinion, reflect essentially stripping in the K , L , and M shells (corresponding to a clustering of α around 2, 1, and 0—see Fig. 3 of Ref. 20).

Our universal formula allows the extraction of one-electron ionization cross sections for a given shell of the ion, either mean cross sections for major shells (Fig. 6) or

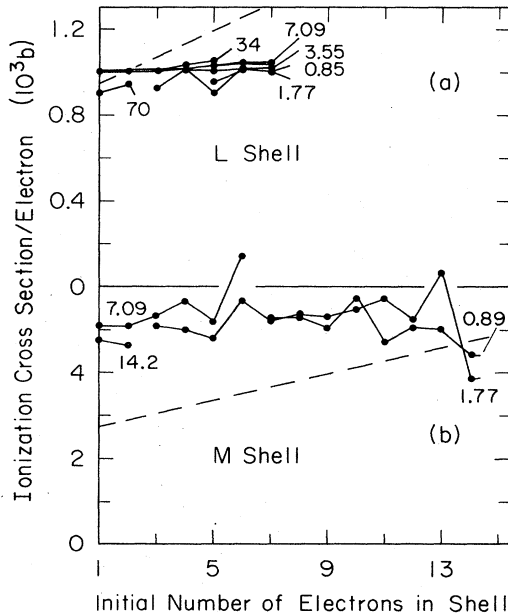


FIG. 7. (a) L -shell one-electron ionization cross sections extracted from 962-MeV/amu $U^{83+} + Mylar$ data using Eq. (23) with $g=0.3$. (b) M -shell one-electron ionization cross sections extracted from 962-MeV/amu $U^{68+} + Mylar$ data using Eq. (23) with $g=3$. The abscissa is the number of electrons in the shell being stripped. Points for a given target thickness (shown in mg/cm²) are connected by straight lines to guide the eye. Dashed lines are PWBA predictions.

cross sections as a function of electron number in the shell (Fig. 7). Comparison with PWBA theory does not give particularly good agreement, perhaps due to excited-state effects⁴ which we hope to consider in a future global treatment of charge-state distributions of relativistic ions passing through solid targets.

ACKNOWLEDGMENTS

We are very grateful to H. Gould for making available to us unpublished charge distributions and for encouraging the present investigation. We thank all our collaborators in the Xe and U charge-state measurements, H. Gould, Ch. Munger, B. Feinberg, R. M. MacDonald, and J. Alonso from Lawrence Berkeley Laboratory and H. E. Wegner and P. Thieberger from Brookhaven National Laboratory. This work was supported in part by the National Science Foundation under Grant No. PHY 83-13676.

APPENDIX: IONIZATION CROSS SECTION

The plane-wave Born approximation ionization cross sections were computed as described in Ref. 7. For the longitudinal part of the cross section, various tabulations of reduced cross sections are available.^{21–25} Contrary to the suggestion in Ref. 7, the cross sections were not multiplied by the factor given in Eq. (23) of that reference, since reconsideration of the theoretical expressions using Dirac wave functions showed that this factor is not justified at relativistic velocities. For the transverse part of the K -shell cross section, Eq. (24) of Ref. 7 was used. For the ratio of the transverse to the longitudinal part of the L -shell cross section, we used the approximate expression²⁶

$$1 + (\ln\gamma^2 - \beta^2) / \ln(2mc^2\beta^2/U_L),$$

where $\beta=v/c$, $\gamma=(1-\beta^2)^{-1/2}$, m is the rest mass of electron, U_L is the L -shell binding energy, and v is the projectile velocity. For the M shell, the transverse part of the cross section was neglected.

In Ref. 21, the (longitudinal) ionization cross section for the shell s is expressed in the form

$$\sigma_i^s = 8\pi a_0^2 Z^2 Z_s^{-4} f_s \eta_s^{-1}, \quad (A1)$$

where a_0 is the Bohr radius of hydrogen, Z is the charge of the ionizing collision partner (in our case, the target), Z_s is the screened charge of the partner which is ionized (in our case, the projectile), and f_s is a function which depends on the velocity parameter η_s and on the screening parameter θ_s :

$$\eta_s = \beta^2 / (Z_s \alpha)^2, \quad (A2)$$

$$\theta_s = s^2 U_s / Z_s^2 R. \quad (A3)$$

Here, α is the fine-structure constant, U_s is the ionization potential of the shell s , and R is the Rydberg constant in energy units.

For Z we used the unscreened target charge, since at the high velocities of interest here screening effects are less than $\sim 10\%$ even for the M shell.²⁷ To compute Z_s ,

we used Slater screening constants.²⁸ The values of I_s were taken from Ref. 15.

A useful interpolation formula for f in the η range (≥ 1) of interest here was found to be

$$f_s = a\theta_s^{-p}(\ln\eta_s + b). \quad (\text{A4})$$

This formula is somewhat simpler, but less accurate, than one given in Ref. 23. It turns out that p has a value close to 1.5 independent of s , but a and b vary with s and with the range of η_s and θ_s considered.

We included the polarization and binding corrections proposed by Basbas, Brandt, and co-workers for the im-

mediate velocity range.^{14,23} A simple estimate of these corrections, using Eq. (A4), is given by

$$\sigma_i^s(\text{corr}) = \zeta^{-p}\sigma_i^s, \quad (\text{A5})$$

where the function ζ is given in Refs. 14 and 29. For the projectile and target combinations considered here, the extreme values of ζ^{-p} are ~ 1.1 , ~ 0.8 , and ~ 1.1 for the K , L_1 , and $L_{2,3}$ shells, respectively. Although we feel less certain about the formulation of the relativistic-electron correction proposed in Ref. 29, we did apply it. It decreases the U K -ionization cross sections by at most $\sim 10\%$, and the L cross sections by at most $\sim 3\%$.

*Permanent address: Department of Physics, Tsinghua University, Beijing, People's Republic of China.

¹R. Anholt, Phys. Rev. A 31, 3579 (1985) (Paper II).

²W. E. Meyerhof, R. Anholt, H. Gould, Ch. Munger, J. Alonso, P. Thieberger, and H. E. Wegner, Phys. Rev. A 32, 3291 (1985) (Paper III).

³R. Anholt, W. E. Meyerhof, H. Gould, Ch. Munger, J. Alonso, P. Thieberger, and H. E. Wegner, Phys. Rev. A 32, 3302 (1985) (Paper IV).

⁴R. Anholt and W. E. Meyerhof, Phys. Rev. A 33, 1556 (1986) (Paper V).

⁵R. Anholt, W. E. Meyerhof, Xiang-Yuan Xu, H. Gould, B. Feinberg, R. M. MacDonald, H. E. Wegner, and P. Thieberger (Paper VIII) (unpublished).

⁶H. D. Betz, Rev. Mod. Phys. 44, 465 (1972).

⁷R. Anholt, Phys. Rev. A 19, 1004 (1979) and references given therein.

⁸J. Eichler, Phys. Rev. A 32, 112 (1985).

⁹N. Bohr and J. Lindhard, K. Dan. Vidensk. Selsk. Mat.-Fys. Medd. 28, No. 7, 1 (1954).

¹⁰W. E. Meyerhof, R. Anholt, Xiang-Yuan Xu, H. Gould, B. Feinberg, R. M. MacDonald, H. E. Wegner, and P. Thieberger, (unpublished). In this paper, we point out that the Auger effect accompanying L -shell vacancy formation can produce an apparent increase in the projectile M -shell multiple-ionization cross sections, especially for low- Z targets. Nevertheless, this effect does not influence significantly the global charge-state distributions considered in the present paper.

¹¹V. S. Nikolaev, Usp. Fiz. Nauk 85, 679 (1965) [Sov. Phys.—Usp. 8, 269 (1965)].

¹²H. Gould, D. Greiner, P. Lindstrom, T. J. M. Symons, and H. Crawford, Phys. Rev. Lett. 52, 180 (1984), and private communications.

¹³S. Datz, H. O. Lutz, L. B. Bridwell, C. D. Moak, H. D. Betz, and L. D. Ellsworth, Phys. Rev. A 2, 430 (1970).

¹⁴G. Basbas, W. Brandt, and R. Laubert, Phys. Rev. A 17, 1655 (1978).

¹⁵T. A. Carlson, C. W. Nestor, Jr., N. Wasserman, and J. D. McDowell, At. Data 2, 63 (1970).

¹⁶V. O. Kostroun, in *X-Ray and Atomic Inner-Shell Physics—1982*, edited by B. Crasemann (AIP, New York, 1982), p. 303.

¹⁷H. Bateman, Proc. Cambridge Philos. Soc. 40, 423 (1910).

¹⁸T. Åberg and O. Goscinski, Phys. Rev. A 24, 801 (1981).

¹⁹O. Goscinski, T. Åberg, and M. Peltonen, Phys. Lett. 90A, 464 (1982).

²⁰A. Blomberg, T. Åberg, and O. Goscinski, J. Phys. B 19, 1063 (1986).

²¹G. S. Khandelwal, B. Choi, and E. Merzbacher, At. Data 1, 103 (1969).

²²B. H. Choi, E. Merzbacher, and G. S. Khandelwal, At. Data 5, 291 (1973).

²³R. Rice, G. Basbas, and F. D. McDaniel, At. Data Nucl. Data Tables 20, 503 (1977).

²⁴O. Benka and A. Kropf, At. Data Nucl. Data Tables 22, 219 (1978).

²⁵D. E. Johnson, G. Basbas, and F. D. McDaniel, At. Data Nucl. Data Tables 24, 1 (1979).

²⁶R. Anholt, W. E. Meyerhof, Ch. Stoller, E. Morenzoni, S. A. Andriamonje, J. D. Molitoris, O. K. Baker, D. H. H. Hoffmann, H. Bowman, J.-S. Xu, K. Frankel, D. Murphy, K. Crowe, and J. O. Rasmussen, Phys. Rev. A 30, 2234 (1984).

²⁷R. Anholt, Phys. Lett. 114A, 126 (1986), and unpublished results.

²⁸J. C. Slater, *Quantum Theory of Atomic Structure* (McGraw Hill, New York, 1960), Vol. I, p. 369.

²⁹W. Brandt and G. Lapicki, Phys. Rev. A 29, 465 (1979).